Electronic Journal of Structural Engineering

Original Article

Cite this: DOI:10.56748/ejse.26882

Received Date:12 September 2025
Accepted Date: 19 May 2026

1443-9255
https://ejsei.com/ejse

Coupled Dynamic Response of Multi-Story Suspended Floors System under Multidimensional Seismic Excitation Considering Soil-Structure Interaction

Qingguang He [a,b], Zihao Zhou [a*], Chuanzhi Sun [c]

[a] Key Laboratory of Disaster Prevention and Mitigation in Civil Engineering of Gansu Province, Lanzhou University of Technology, Lanzhou, 730050, China
[b] Western Engineering Research Center of Disaster Mitigation in Civil Engineering of Ministry of Education, Lanzhou University of Technology, Lanzhou, 730050, China
[c] School of Civil Engineering and Architecture, Suqian College, Suqian, 223800, China
* Corresponding author: zzh112233abc@163.com

Abstract

To investigate the multidimensional seismic response of a multi-story suspended floors system considering soil-structure interaction (SSI), a three-dimensional finite element model was established in ABAQUS. Displacement, acceleration, and hanger rod stress responses under near-field pulse-like (NF-P), near-field non-pulse-like (NF-NP), and far-field (FF) ground motions were analyzed, with a focus on the coupling effects of the vertical seismic component. Results show that SSI prolongs structural periods, especially in higher modes. The vertical seismic component nonlinearly amplifies vertical responses: under NF-P ground motion with a PGA of 0.5 g, mean vertical displacement and acceleration of the main structure increase by 2.64 and 2.8 times, respectively, compared to horizontal-only excitation. The acceleration of suspended floor slabs shows even greater sensitivity, with amplification up to 5.05 times. Hanger rods mean stress increases by 19% due to vertical seismic input. These findings highlight the necessity of incorporating SSI and vertical seismic effects into design codes for suspended structures, especially in near-fault regions, to improve the structural safety and seismic performance of such structures.

Keywords

Multi-story suspended floors system, Soil-structure interaction, Multidimensional seismic excitation, Near-field pulse-like ground motion, Dynamic response

1. Introduction

Suspended structures, as an innovative architectural form, have gained engineering applications in public buildings in recent years (Xiao et al., 2022; Liang et al., 2025). This structural system utilizes hangers (cables) to suspend all or partial floors from the main structure, leveraging the excellent tensile properties of steel. During earthquakes, the suspended dissipate energy through swinging motions, protecting the structure while exhibiting self-centering capabilities under gravity. Practical seismic damage observations confirm the superior vibration reduction performance of suspended structures, along with advantages in architecture, construction, and materials.

Research on the seismic behaviour of suspended structures has progressed along three interrelated directions: the formulation of analytical and numerical models of vibration reduction, experimental validation through shaking table testing, and the development of innovative configurations and parameter-optimisation strategies for enhanced control performance.

Early analytical work focused on establishing reliable simplified representations of the dynamic response of suspended systems. Comparative response-spectrum analyses showed that few-degrees-of-freedom representations tend to overestimate internal forces and displacements relative to multi-segment multi-layer models (Guo et al., 2003), motivating the use of higher-fidelity formulations in design. Subsequent theoretical and finite element studies systematically characterised the influence of mass and frequency ratios between the main structure and the suspended substructure (Wei et al., 2013), confirming that, with appropriate parameter tuning and the integration of isolation bearings, suspended systems can achieve markedly improved vibration mitigation under dynamic excitation.

These analytical findings have been corroborated by extensive shaking table experiments. Investigations of suspended core-tube systems for high-rise buildings consistently report lower fundamental frequencies and enhanced energy dissipation compared with conventional frame core-tube configurations, with strong agreement between numerical predictions and experimental measurements (Zhou et al., 2005a, 2005b; Cao et al., 2007). More recent shaking table tests on a 1/20 scaled two-segment 19-story mega-frame suspended structure further demonstrated that the suspended floors act as additional mass for the main structure and dissipate energy through swinging motions, and that replacing rigid connecting rods with viscous dampers substantially enhances the overall energy dissipation capacity (Du et al., 2022).

In parallel, considerable effort has been devoted to innovative system configurations and parameter-optimisation strategies. A semi-flexible suspended system has been proposed and supported by closed-form equations of motion and stochastic response expressions, together with parametric optimisation of damper stiffness, damping coefficients, and the location of the flexible segments (Wang et al., 2008a, 2008b). A multi-story suspended floors system has been developed and analysed (He et al., 2020), demonstrating superior seismic resistance under strong ground motions and the benefits of optimising key structural parameters. Multi-objective genetic algorithms have been employed to optimise the vertical distribution of substructure parameters in modularised suspended structures, yielding improved robustness and multi-mode control performance (Ye et al., 2019). A closely related line of research treats the suspended floors themselves as tuned mass dampers (TMDs): suspended floor systems with replaceable energy-dissipation elements (Mahmoud and Chulahwat, 2015), and combinatorial optimisation of slab distribution, damping ratios, and frequency ratios under combined wind and seismic excitations (Chulahwat and Mahmoud, 2017), have both been shown to deliver effective multi-hazard vibration control.

Taken together, these studies provide a solid foundation for the seismic design of suspended structures, yet two limitations recur across them. First, with few exceptions, attention has been confined to the horizontal seismic response, leaving the vertical dynamic behaviour of suspended structures largely unexplored, even though the flexibly connected substructures are intrinsically sensitive to vertical excitation. Second, the foundation has typically been treated as rigid, so that the modifying role of the underlying soil on the dynamic characteristics of suspended systems remains insufficiently understood.

Most studies on soil-structure interaction (SSI) have primarily focused on high-rise buildings and underground structures (Yang et al., 2024; Islam et al., 2024; Yang et al., 2024; Abdelhalim et al., 2025), however, the influence of SSI remains underexplored in current research on suspended structures. Moreover, actual seismic events occur in three-dimensional space, involving both horizontal and vertical ground motion components. The flexible connections between suspended substructures and the main structure introduce vertical dynamic characteristics, where vertical seismic excitations may induce significant displacements and acceleration responses in suspended components, potentially compromising structural

stability and safety. Currently, the horizontal seismic behavior of suspended structures has been extensively studied (Ye et al., 2020; Liu et al., 2022; Chen et al., 2023), while investigations into their performance under multi-directional seismic actions remain limited. Therefore, it is imperative to develop numerical models that fully incorporate soil-suspended structure dynamic interactions and systematically analyze their seismic responses under multi-directional excitations, thereby providing theoretical foundations for the seismic design of suspended structures.

This study's key innovations and principal contributions are summarized as follows: (1) It establishes a comprehensive 3D finite element model of multi-story suspended floors system considering SSI, filling the gap of insufficient integration of SSI in existing suspended structures research. (2) It systematically analyzes the coupling effects of vertical seismic component and SSI under three types of ground motions, revealing the nonlinear amplification mechanism of vertical responses. (3) It quantifies the influence of SSI on structural dynamic characteristics and seismic responses, providing precise data support for seismic design of suspended structures in near-fault regions.

2. Structural Modeling

2.1 Structural Configuration

This study investigates a multi-story suspended floors system (Yin, 2020), as illustrated in Fig.1. The proposed system is conceptually a Multiple Tuned Mass Damper (MTMD) system characterized by the vertical distribution of TMD units along the structural height. This configuration plays a critical role in enhancing the seismic resilience of structures, as the vertically distributed MTMDs effectively mitigate structural vibrations through a passive control mechanism (Naderpour et al., 2024; Ozturk et al., 2022; Pasand et al., 2024).

Unlike conventional suspended systems, rigid connections are retained solely between the rooftop beams and columns to prevent beam-column joint damage, while suspension points for the suspended floor slabs are positioned along the columns and linked via connectors and suspension utilizes hanger rods. To compensate for the stiffness reduction caused by the removal of partial beam-column joints, bracing systems are implemented between columns to maintain structural stability. Additionally, buffer devices (springs and dampers) are installed in the gaps between the suspended floor beams and columns to enhance self-centering capacity and energy dissipation performance. These devices provide elastic restraint to limit displacement amplitudes of the suspended floor slabs and prevent collisions through stiffness regulation, while simultaneously dissipating seismic energy via damping mechanisms to improve system self-centering capacity.

2.2 Model Parameters

A three-dimensional finite element model of a suspended structural system incorporating soil-structure interaction is developed using the finite element software ABAQUS 2023. The structure is designed as a five-story steel frame, where all stories except the top roof level are suspended substructures. Each story has a height of 3.6 m, yielding a total building height of 18 m. Floor beams and bracing members utilize I-shaped steel sections, while columns are constructed with box-section steel sections. Floor slabs consist of 120 mm-thick composite slabs, and suspension hanger rods are fabricated from 30 mm-diameter round steel bars. The foundation system employs a 7 m × 7 m reinforced concrete raft foundation. The overall model configuration is illustrated in Fig. 2, with component cross-sections, types, and geometric dimensions detailed in Table 1.

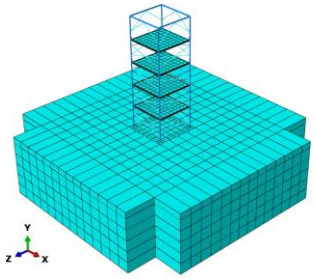

Fig. 2 Finite element model of suspended structures considering SSI

Table 1. Component cross-section types and dimensions

Component type	Length (mm)	Cross-section (mm)
Column	3600	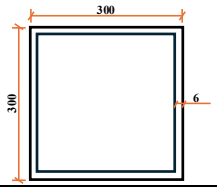
Rooftop beam	6000	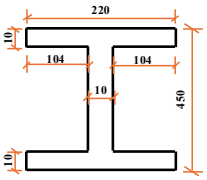
Top bracing	3800	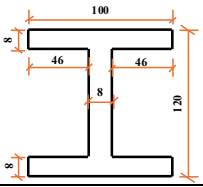
Cross bracing	6200	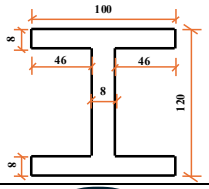
Suspension hanger rod	500	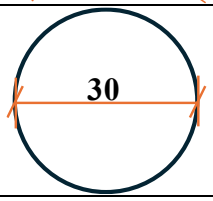

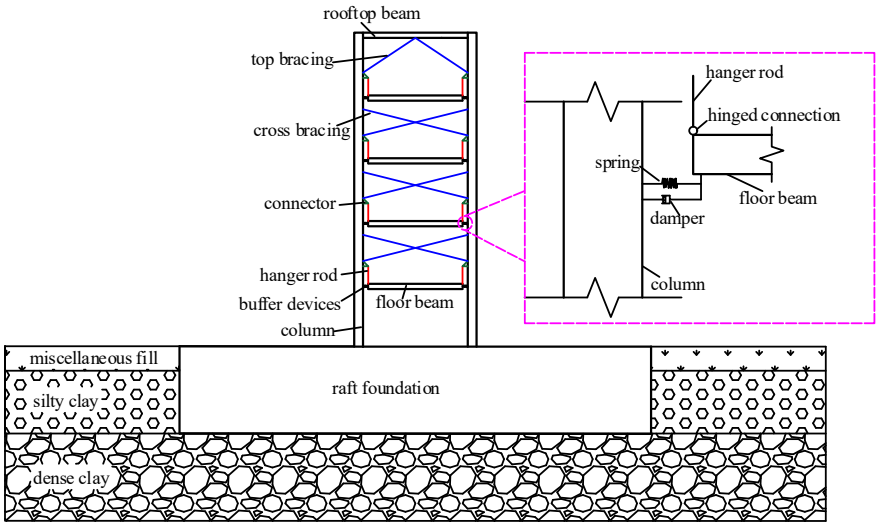

Fig. 1 multi-story suspended floors system

The finite element mesh was designed following the principle that the element size should be less than one-eighth to one-tenth of the minimum wavelength of the propagating seismic waves. Based on the shear wave velocities of the soil layers (ranging from 183.7 to 244.9 m/s) and the dominant frequencies of the input ground motions (0.25-12.35 Hz), the minimum wavelength in the soil domain is approximately 15 m. The soil domain was discretized with element sizes of 1.75 m to 1.9 m in the near-field region surrounding the foundation, and 5.0 m in the far-field region approaching the boundaries. The near-field mesh refinement ensures accurate capture of stress concentration and soil-structure interaction effects, while the coarser far-field mesh reduces computational cost without compromising accuracy. The soil domain extends 36 m × 36 m in plan (approximately 5 times the 7 m foundation width) and 10 m in depth, following recommendations from previous SSI studies (Lu et al., 2007) to minimize boundary effects on structural response.

The soil is discretized using three-dimensional infinite elements (CIN3D8), with infinite domain characteristics simulated via the infinite element boundary method. The main structural frame, including columns, beams, and braces, is discretized using beam elements (B31), while the suspended floor slabs are discretized with shell elements (S4R). Contact between the soil and suspended structure is defined using a master-slave contact surface, with hard contact enforced in the normal direction and a Coulomb friction model applied in the tangential direction.

Contact between the soil and suspended structure is defined using a master-slave contact surface approach, where the foundation structure is designated as the master surface and the surrounding soil as the slave surface. In the normal direction, "hard contact" is enforced, allowing separation when tensile stresses develop while preventing penetration under compression. In the tangential direction, a Coulomb friction model is applied with a friction coefficient of 0.4, which was determined based on the interface properties between concrete and silty clay as specified in geotechnical engineering guidelines. This contact formulation enables simulation of pile-soil separation, sliding, and foundation uplift phenomena that may occur during strong ground motions. The energy dissipation at the soil-structure interface during dynamic interaction is accounted for through the Rayleigh damping components incorporated in the contact elements.

The superstructure and foundation materials in the model adopt a linear elastic constitutive model, with the main structure constructed from Q345 steel and the raft foundation from C50-grade reinforced concrete. The soil constitutive model employs linear elastic theory combined with the Mohr-Coulomb plasticity model, incorporating the Von Mises hardening rule to characterize soil nonlinearity, and the soil parameters of the site are detailed in Table 2. The damping model uses the Rayleigh damping model, with the damping coefficients α and β calculated based on the first two natural frequencies obtained from the modal analysis.

The superstructure and foundation materials in the model adopt a linear elastic constitutive model, with the main structure constructed from Q345 steel and the raft foundation from C50-grade reinforced concrete. The steel material follows a bilinear kinematic hardening model with a hardening modulus of 0.01E to capture the nonlinear behavior under strong ground motions.

The soil constitutive model employs linear elastic theory combined with the Mohr-Coulomb plasticity model, incorporating the Von Mises hardening rule to characterize soil nonlinearity. This modeling approach was selected for several reasons: (1) The Mohr-Coulomb model is widely validated for cohesive-frictional materials and can adequately capture the shear failure mechanism of clay soils under seismic loading; (2) It requires fewer material parameters compared to advanced constitutive models (such as the Drucker-Prager or Cam-Clay models), which can be reliably obtained from standard geotechnical tests; (3) Previous studies on soil-structure interaction have demonstrated that the Mohr-Coulomb model provides reasonable predictions of structural responses when the primary concern is the overall dynamic behavior rather than detailed soil deformation patterns.

Table 2. Soil properties parameters of the foundation soil

Soil layer	Thickness (m)	Elastic modulus (MPa)	Poisson's Ratio	Cohesion (MPa)	Friction angle (°)	Density (kg/m³)	Shear wave velocity (mm/s)
Miscellaneous fill	1.4	152.1	0.38	0.05	15.5	1801	1.837×10^5
Silty clay	3.6	253.9	0.32	0.013	23.0	1922	2.143×10^5
Dense clay	5.0	316.9	0.30	0.020	30.0	1980	2.449×10^5

The buffer devices connecting the suspended floor slabs and the main structure columns are modeled using spring-damper elements. Based on optimization studies for suspended structure systems (He et al., 2020), the spring stiffness coefficient is set to 2.0×10^4 N/m, and the viscous damping coefficient is set to 3.0×10^3 N·s/m.

The damping of the system is represented by the Rayleigh damping model, in which the damping matrix $[C]$ is expressed as a linear combination of the mass matrix $[M]$ and the stiffness matrix $[K]$, as given in Eq. (1):

$$[C] = \alpha[M] + \beta[K] \quad (1)$$

where α and β are the mass-proportional and stiffness-proportional damping coefficients, respectively. For the soil–structure interaction system, separate coefficients are evaluated for the soil and structural subsystems using their respective first two natural circular frequencies, ω_1 and ω_2, obtained from modal analysis. The coefficients are determined from Eq. (2) and Eq. (3):

$$\alpha = \frac{2\xi\omega_1\omega_2}{\omega_1+\omega_2} \quad (2)$$

$$\beta = \frac{2\xi}{\omega_1+\omega_2} \quad (3)$$

where ξ is the target damping ratio. A damping ratio of 2% is adopted for the steel structure, whereas 5% is used for the soil domain to account for the higher material damping of soils. This substructure treatment allows the classical damping assumption to be applied appropriately to the inherently non-classical soil–structure interaction system.

2.3 Model Validation

Based on the scaled experimental model from Lu et al., (2007), this study develops a corresponding finite element model using ABAQUS software. Modal analysis is conducted to extract the natural frequencies of the structure, and the numerical results are validated against experimental data provided in Lu et al., (2007), with quantitative comparisons detailed in Table 3. The data indicates a maximum discrepancy of 8.65% between simulations and experiments when SSI is considered. This discrepancy demonstrates the applicability of the proposed model in simulating SSI within practical structural systems. It should be noted that the validation in this study follows the same approach adopted in the original reference (Lu et al., 2007), where frequency comparison was used as the primary validation metric due to the nature of field-testing conditions. This approach is consistent with established practices in SSI research, where modal parameters serve as fundamental indicators of system dynamic characteristics (Chopra., 2017; Wolf., 1985). The accurate prediction of natural frequencies, particularly the first-mode frequency (error of 3.26%), indicates that the model correctly captures the essential stiffness and mass distribution of the soil-structure system.

For completeness, the prototype experiment of Lu et al. (2007) is briefly described here so that the present validation can be assessed independently. That study reported a large-scale (1:2) cast-in-place soil–pile–structure field model built on a natural site. The superstructure was a seven-story reinforced-concrete frame without infill walls, with a 3.0 m × 3.0 m column grid and a total height of 12.0 m (first-story height 2.1 m, the remaining stories 1.65 m each); the measured concrete grade of the slabs was C40. The structure was supported on a pile foundation comprising piles of approximately 7.0 m length and 350 mm diameter, capped by 750 mm × 750 mm pile caps tied by foundation beams. The site profile, from the surface downward, consisted of fill, hard-plastic silty clay, residual silty clay, and strongly-to-moderately weathered argillaceous slate; in-situ shear-wave-velocity tests and laboratory tests classified the site as a medium-soft, Class II site. The model was tested underground pulsation measurements, top traction (free-vibration) excitation, and top mechanical (forced-vibration) excitation, under three counterweight conditions (gravity-neglected, under-artificial-mass, and artificial-mass), from which the dynamic response and the first two natural frequencies of the system were extracted. The prototype field model is shown in Fig. 3.

Fig. 3 Large-scale (1:2) soil–pile–structure field model used for validation (after Lu et al., 2007)

Table 3. Comparison of natural frequencies between the finite element model and the scaled experimental model

Frequency	Simulation value (Hz)	Scaled model test data					
		Calculated value (Hz)	Error (%)	Top traction excitation (Hz)	Error (%)	Top mechanical excitation (Hz)	Error (%)
First Mode	1.932	1.995	3.26	1.843	4.61	1.900	3.09
Second Mode	6.071	6.596	8.65	6.250	2.95	6.200	2.67

2.4 Modal Comparison

During the modal analysis, the contact between foundation and soil is defined as a tie constraint, with the degrees of freedom at the soil base fully restrained. Due to the significant stiffness contrast between the soil and structure, performing modal analysis directly may lead to coupling between local vibrations of the soil and structural vibrations, thus interfering with the extraction of dynamic characteristics. To address this, the soil mass is neglected by assigning zero mass to the soil, retaining only its constraint effects on the structure, and the first four mode shapes of the SSI system are obtained. A comparison of natural periods between two models (with and without SSI) is presented in Table 4. It can be observed that the natural periods of the first few mode shapes are very close. However, when SSI is considered, the soil constraints reduce the equivalent lateral stiffness of the structure, leading to increased natural periods. This period increment becomes more pronounced for higher modes.

Table 4. Period comparison

Mode shape	Period (s)	
	Without SSI	With SSI
1st mode	1.7628	1.8429
2nd mode	1.7482	1.8282
3rd mode	1.7473	1.8273
4th mode	1.5601	1.7471

To conduct a more in-depth analysis of the impact of SSI on the dynamic characteristics of the structure, Figures 4 and 5 present a comparison of the first four mode shapes for the suspended structural system both without and with SSI. As observed in the deformation patterns of the first four modes in Fig. 5, all modes are characterized by horizontal translational displacements of the suspended substructures, consistent with the kinematic deformation mechanisms of suspended structures. Modal analysis of the structure indicates that the deformation is primarily characterized by horizontal displacements of the suspended floors, while the main structure exhibits minimal displacement.

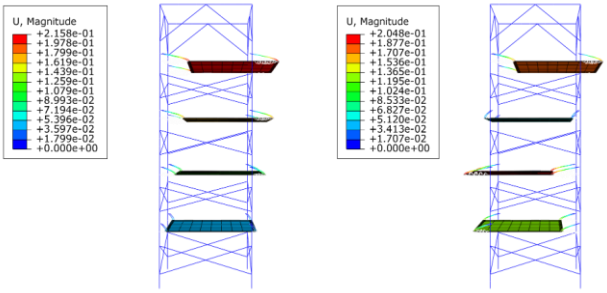

X-Translational (a) 1st mode Y-Translational (b) 2nd mode

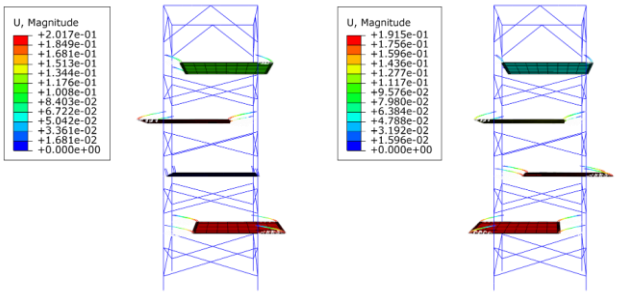

X-Translational (c) 3rd mode Y-Translational (d) 4th mode

Fig. 4 Mode shape diagram of suspended structure neglecting SSI

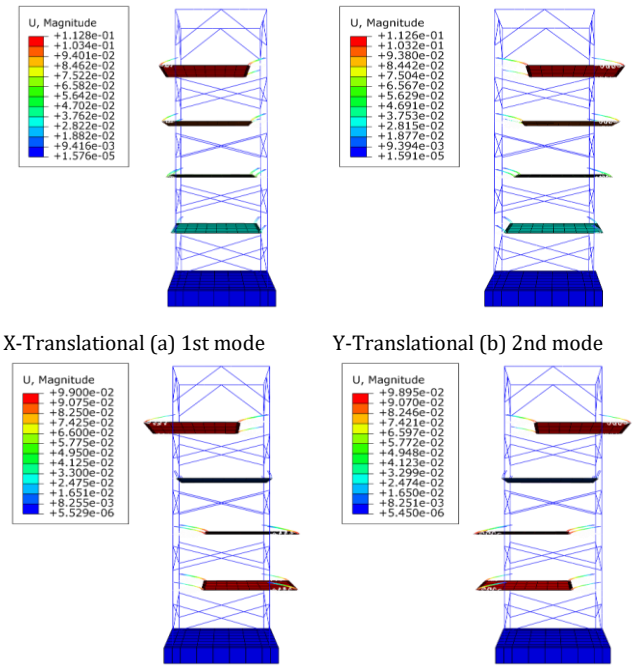

X-Translational (a) 1st mode Y-Translational (b) 2nd mode

X-Translational (c) 3rd mode Y-Translational (d) 4th mode

Fig. 5 Mode shape diagram of suspended structure considering SSI

3. Selection of Seismic Waves

Following the recommendations outlined in the FEMA P695 report (FEMA, 2009), this study selects appropriate ground motion records for structural seismic analysis based on the following criteria: (1) seismic events with magnitudes larger than M 6.5; (2) ground motions considering the source mechanism of strike-slip faults; (3) records from Site Class C and D to be consistent with the site conditions of the investigated structure; and (4) a minimum effective period of 14 seconds to cover potential structural vibration frequencies. This screening process ensures that the selected ground motions provide representative and rational inputs for engineering analysis. The nine selected ground motion records, all sourced from the Pacific Earthquake Engineering Research Center (PEER) database, are listed in Table 5.

Figure 6 presents the acceleration time history curves and Fourier spectra of the three selected ground motions. The near-field pulse-like (NF-P) ground motions exhibit frequency components primarily distributed within 0.1-5 Hz, with a mean dominant frequency of 0.61 Hz. The near-field non-pulse-like (NF-NP) ground motions show frequency components concentrated in 0.5-7.6 Hz, with a mean dominant frequency of 3.19 Hz. In contrast, the far-field (FF) ground motions are predominated by frequencies in the 5-22 Hz range, with a mean dominant frequency of 9.06 Hz. This indicates that FF ground motions are characterized by richer high-frequency components, while both NF-P and NF-NP ground motions predominantly occupy the mid-to-low frequency ranges.

For comparative purposes, the peak ground accelerations (PGA) of the three ground motions are scaled to 1 g, and their normalized acceleration response spectra are plotted in Fig. 7. In this study, the first natural period of the suspended structural system considering SSI is 1.84 s. Consequently, under NF-P ground motions, the structural acceleration responses are amplified compared to those under NF-NP and FF ground motions. Additionally, NF-P ground motions exhibit strong velocity pulse effects, characterized by abrupt energy input within a short period of time and generation of higher acceleration responses in the longer period range, which may induce more severe structural damage. Therefore, it is imperative to conduct a more detailed investigation into the dynamic responses of suspended structures under different types of ground motions, particularly NF-P ground motions.

Table 5. Basic information on seismic motion

Seismic type	Year	Earthquake name	Recording station	Magnitude	Epicentral distance (km)	PGA (g)	Arias Intensity (m/s)	Dominant frequency (Hz)
NF-P 1	1979	Imperial Valley-06	EC County Center FF	6.53	7.31	0.212	0.8	0.73
NF-P 2	1980	Irpinia_Italy-01	Bagnoli Irpinio	6.9	8.14	0.130	0.4	0.86
NF-P 3	2010	Darfield_New Zealand	Riccarton High School	7	13.64	0.190	1.2	0.25
NF-NP 1	1979	Imperial Valley-06	Calexico Fire Station	6.53	10.45	0.277	0.9	2.1
NF-NP 2	1999	Duzce_Turkey	Lamont 1061	7.14	11.46	0.101	0.2	3.08
NF-NP 3	1979	Imperial Valley-06	Parachute Test Site	6.53	12.69	0.113	0.2	4.39
FF 1	2000	Tottori_Japan	OKY007	6.61	41.56	0.094	0.3	6.52
FF 2	2010	Darfield_New Zealand	OXZ	7	33.54	0.126	0.5	8.32
FF 3	2003	Bam_Iran	Abaragh	6.6	47.16	0.169	0.3	12.35

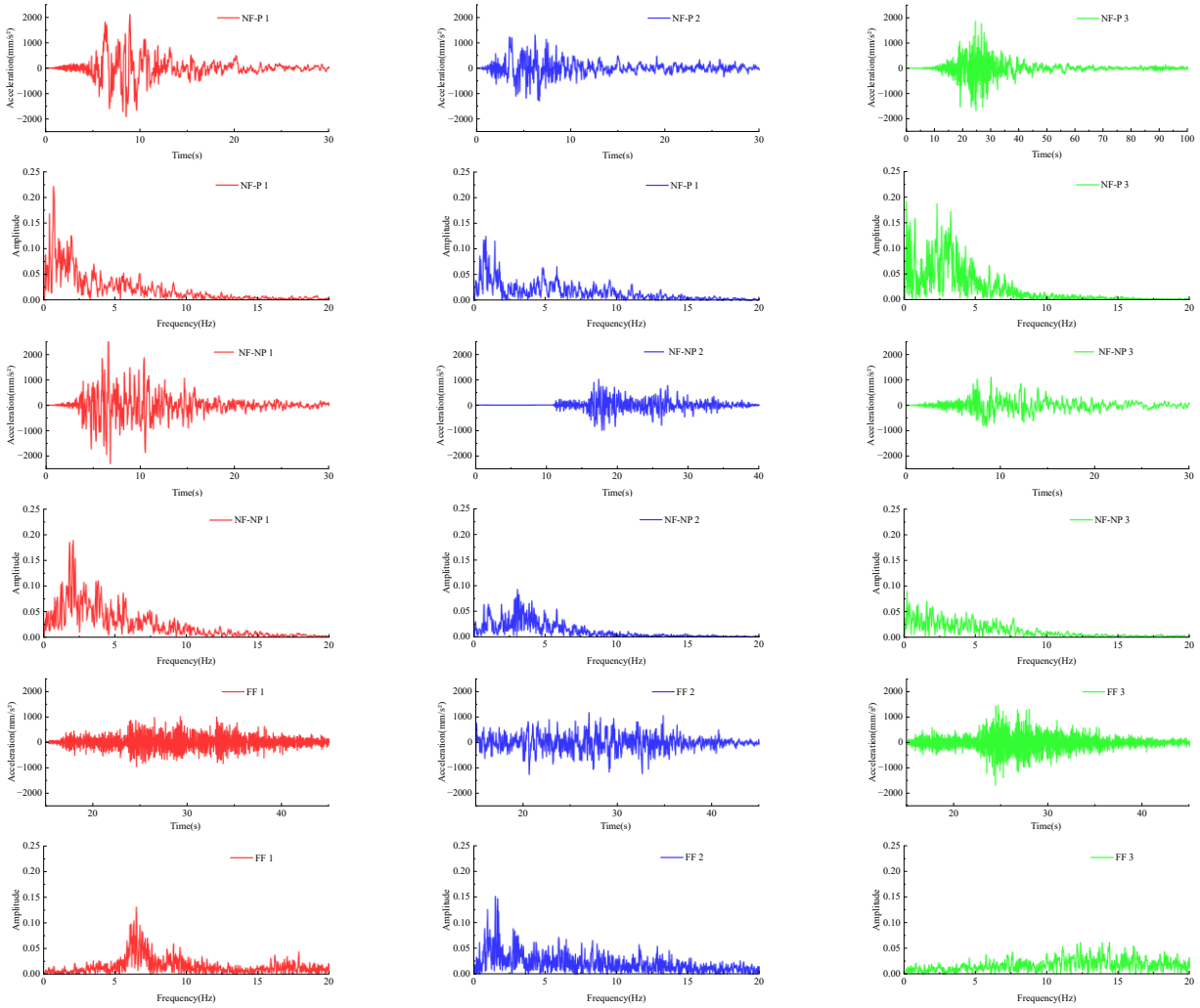

Fig. 6 Seismic acceleration time history curves and Fourier spectra

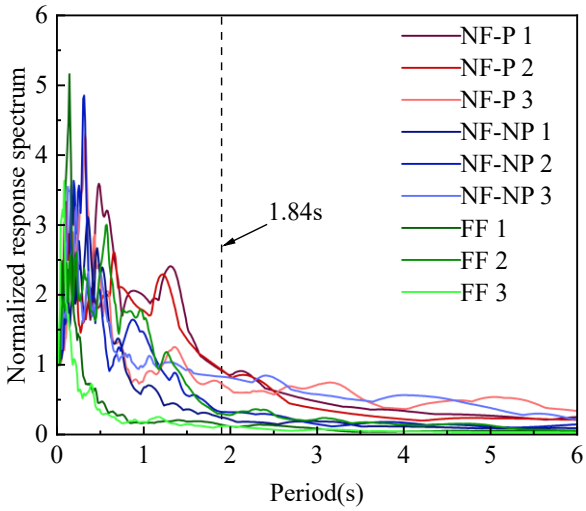

Fig. 7 Acceleration response spectra

4. Structural Dynamic Response

4.1 Main Structural Displacement

The response characteristics of peak displacement at the top floor under horizontal ground motions only and combined horizontal-vertical ground motions (with the vertical component scaled to 0.65 times the horizontal component) (Code for Seismic Design of Buildings. GB 50011-2010) are illustrated in Fig. 8. Analytical results indicate that the vertical seismic component has a limited influence on horizontal top floor displacements. For instance, under NF-P ground motions with a PGA of 0.5 g, the mean horizontal top floor displacement considering vertical seismic effects reaches 263.66 mm, 1.28 times that under horizontal motions alone. Similarly, the corresponding increase in displacement is 1.2 times under NF-NP ground motions and slightly rises to 1.18 times under FF ground motions. This demonstrates that horizontal displacements of the suspended structure are predominantly driven by the horizontal seismic component, with the coupling effects of vertical component not significantly altering the response patterns.

In contrast, the vertical displacement of the suspended structure exhibits significantly higher sensitivity to the vertical seismic component. Under FF ground motions with a PGA of 0.5g, the mean vertical displacement at the top floor considering the vertical seismic component

reaches 1.39 mm, which is 2.01 times that under horizontal seismic excitation alone. Under NF-NP ground motions, the corresponding displacement response increases to 1.97 times, while under NF-P ground motions, the vertical displacement amplification reaches significantly to2.64 times. Comparisons of response differences under various ground motion types reveal that NF-P ground motions, with a mean dominant frequency of 0.61 Hz closely matching the structural natural vibration period of 1.84 s (corresponding frequency: 0.54 Hz), are more likely to induce coupling effects with the structure, resulting in significantly stronger displacement responses compared to far-field ground motions dominated by higher frequencies.

Based on the above analysis, the seismic analysis of multi-story suspended floors system requires particular attention to the vertical seismic component and its correlation with the spectral characteristics of ground motions. Specifically, for ground motions dominated by low-frequency energy, the amplification effect of the vertical component on vertical displacement is significant, necessitating the incorporation of vertical seismic coupling effects into the design process. Although the vertical component has a limited impact on horizontal displacements, careful consideration remains essential under NF-P ground motions to ensure the overall seismic performance of the structure.

4.2 Suspended Floor Slab Displacement

To analyze the influence of multidimensional seismic coupling effects on the dynamic response of the suspended substructures, this study conducts a comparative investigation of the displacement characteristics of the top-floor suspended floor slab under horizontal ground motions alone and combined horizontal-vertical ground motions (with the vertical component scaled to 0.65 times the horizontal component), as shown in Fig. 9. Due to the elevated position of the top-floor suspended floor slab, it is notably affected by higher-mode vibrations, particularly under NF-P ground motions with low-frequency energy input, where resonance tends to occur. Investigating its displacement characteristics is critical for identifying seismic vulnerabilities in the structural system. The results demonstrate that the inclusion of the vertical seismic component has a limited influence on the peak horizontal displacement of the suspended floor slab. At a PGA of 0.5 g, the average increase in horizontal displacement when the vertical component is considered is 1.26 times that under horizontal-only excitation for NF-P, NF-NP, and FF ground motions. In contrast, the vertical displacement of the suspended floor slab exhibits significantly higher sensitivity to the vertical seismic component, with an average displacement increase of 1.52 times. These results reveal that the displacement response of the suspended floor slab under multidimensional seismic inputs varies significantly between directions: horizontal displacements are primarily governed by the horizontal seismic component, whereas vertical displacements are more sensitive to the vertical component. This conclusion provides a basis for refining the design of connection members in suspended substructures.

4.3 Main Structural Acceleration

The peak acceleration response at the top floor of the suspended structure under horizontal ground motions only and combined horizontal-vertical ground motions (with the vertical component scaled to 0.65 times the horizontal component) exhibits distinct variation patterns, as shown in Fig. 10. The inclusion of the vertical seismic component results in a minor change in peak horizontal acceleration but leads to a significant increase in peak vertical acceleration. Under NF-P ground motions with a PGA of 0.5 g, the mean peak horizontal acceleration at the top floor reaches 5364.8 mm/s^2 when the vertical component is considered, which is 1.43 times the peak acceleration under horizontal-only ground motions. Meanwhile, the mean peak vertical acceleration increases to 6475.02 mm/s^2, which is 2.8 times that under horizontal-only excitation. These results indicate that the vertical seismic component significantly amplifies the vertical acceleration response of the suspended structure, necessitating comprehensive consideration of vertical seismic effects in seismic design.

Furthermore, the influence of vertical-to-horizontal (V/H) acceleration amplitude ratios (0.65, 0.85, and 1) of NF-P ground motions on structural responses was investigated in this study. As shown in Fig. 11, under the same peak ground acceleration (PGA), the peak vertical acceleration at the top floor of the suspended structure increases with the V/H ratio. At a PGA of 0.5 g and V/H = 1, the mean peak vertical acceleration reaches 10977.12 mm/s^2, which is 1.7 times the response under V/H = 0.65. Moreover, under the same V/H ratio, the peak vertical acceleration increases with increasing PGA. At V/H = 0.65, the mean peak vertical acceleration at the top floor under a PGA of 0.5 g is 6475.02 mm/s^2, which is 6.34 times that under a PGA of 0.1 g. These observations demonstrate a significant positive correlation between the vertical acceleration response and both the vertical-to-horizontal seismic component ratio (V/H) and the peak ground acceleration (PGA).

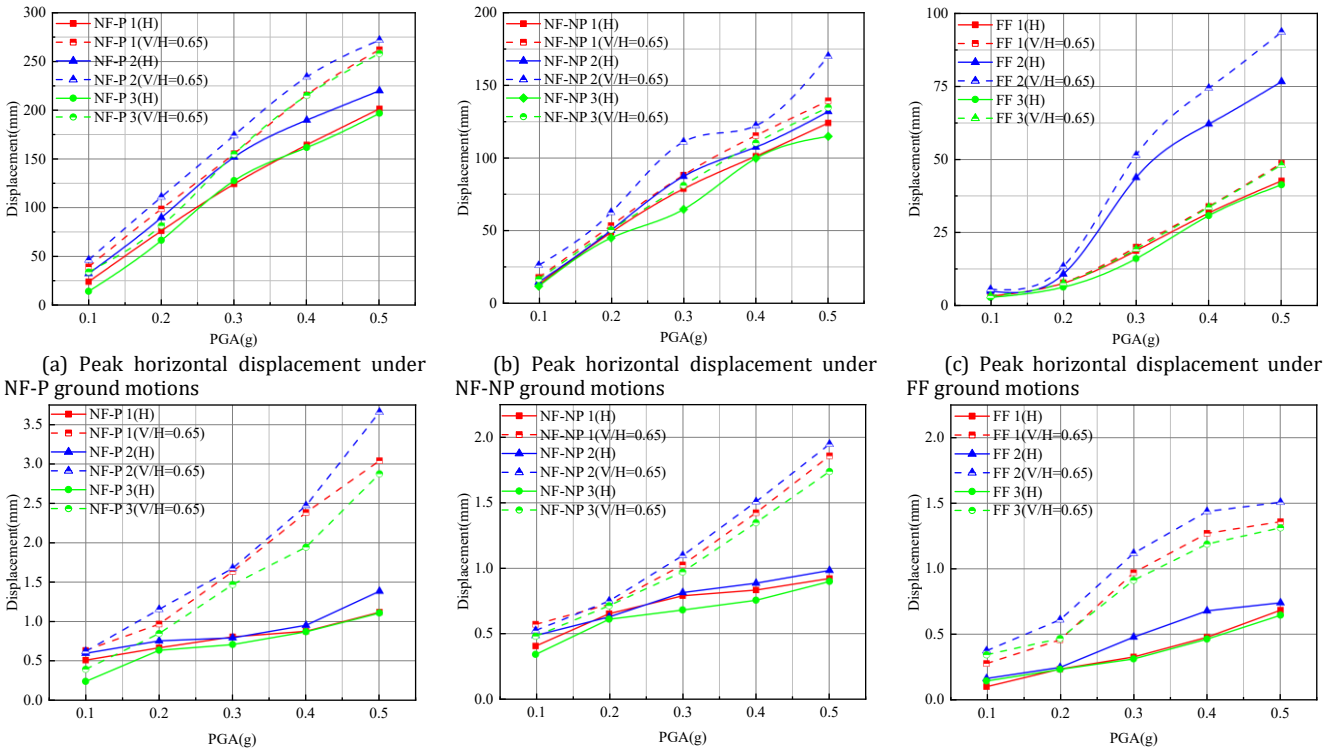

(a) Peak horizontal displacement under NF-P ground motions

(b) Peak horizontal displacement under NF-NP ground motions

(c) Peak horizontal displacement under FF ground motions

(d) Peak vertical displacement under NF-P ground motions

(e) Peak vertical displacement under NF-NP ground motions

(f) Peak vertical displacement under FF ground motions

Fig. 8 Effect of vertical earthquakes on the peak displacement at the top floor

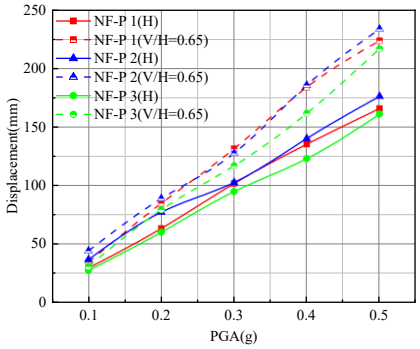

(a) Peak horizontal displacement under NF-P ground motions

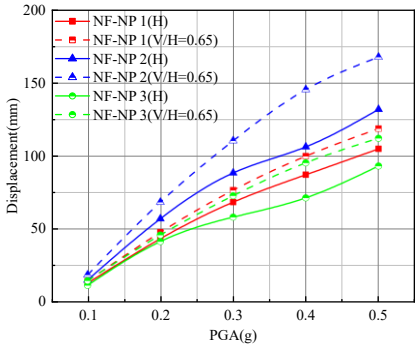

(b) Peak horizontal displacement under NF-NP ground motions

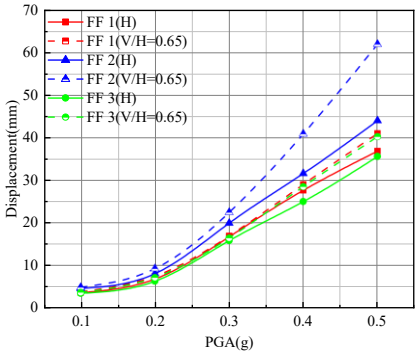

(c) Peak horizontal displacement under FF ground motions

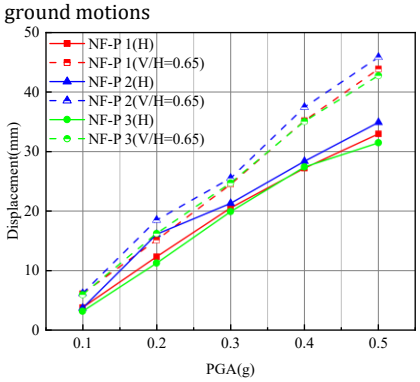

(d) Peak vertical displacement under NF-P ground motions

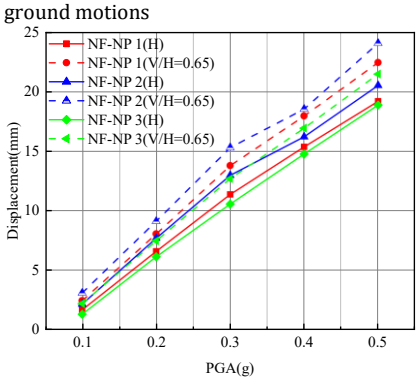

(e) Peak vertical displacement under NF-NP ground motions

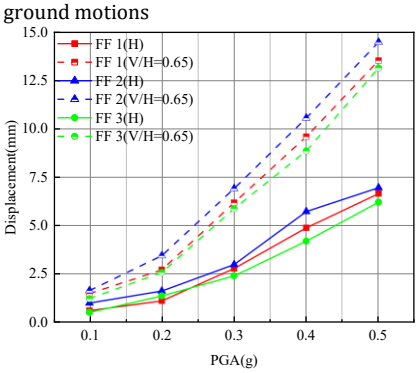

(f) Peak vertical displacement under FF ground motions

Fig. 9 Effect of vertical earthquakes on the peak displacement of the suspended floor slab

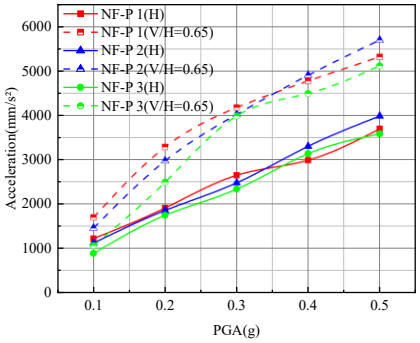

(a) Peak horizontal acceleration under NF-P ground motions

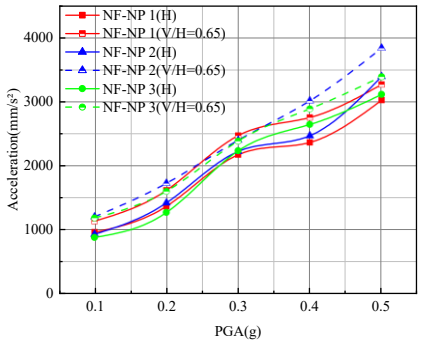

(b) Peak horizontal acceleration under NF-NP ground motions

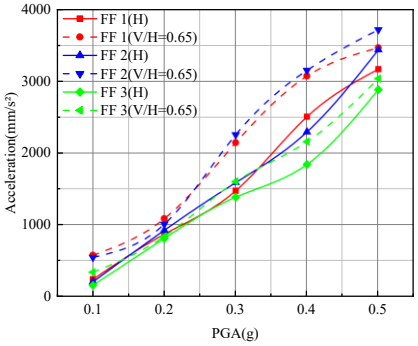

(c) Peak horizontal acceleration under FF ground motions

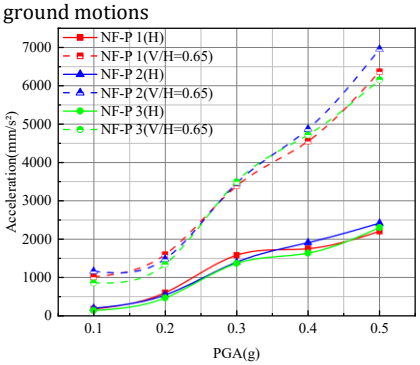

(d) Peak vertical acceleration under NF-P ground motions

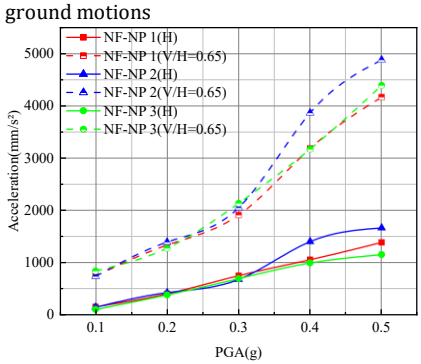

(e) Peak vertical acceleration under NF-NP ground motions

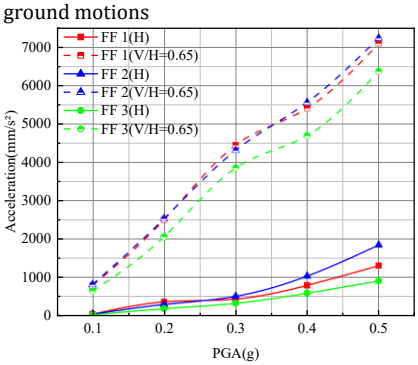

(f) Peak vertical acceleration under FF ground motions

Fig. 10 Effect of vertical earthquakes on the peak acceleration at the top floor

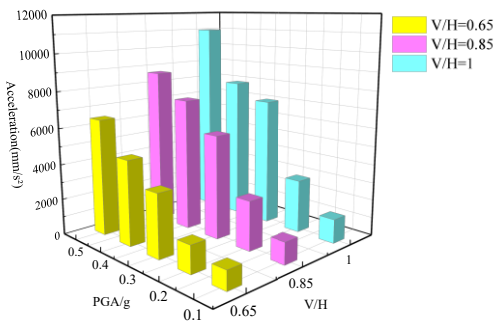

Fig. 11 Effect of the vertical component of near-field pulse-like ground motions on the peak acceleration at the top floor

4.4 Suspended Floor Slab Acceleration

The response characteristics of the peak acceleration at the top-floor suspended floor slab under horizontal ground motions only and combined horizontal-vertical ground motions (with the vertical component scaled to 0.65 times the horizontal component) are illustrated in Fig. 12. The inclusion of the vertical seismic component has a limited influence on the peak horizontal acceleration but significantly amplifies the vertical acceleration response. Under NF-P ground motions with a PGA of 0.5 g, the mean peak horizontal acceleration of the suspended floor slab reaches 5693.37 mm/s^2 when the vertical component is considered, corresponding to 1.73 times the peak horizontal acceleration under horizontal-only excitation. In contrast, the mean peak vertical acceleration increases sharply from 1184.08 mm/s^2 to 5979.77 mm/s^2, representing an increase of 5.05 times. This significant amplification phenomenon is

driven by the combined effect of resonance mechanisms and structural dynamic characteristics, with key contributing factors analyzed as follows:

First, resonance coupling between the NF-P ground motion and the suspended structure is the core driver. The dominant frequency of NF-P ground motions (0.61 Hz) is highly close to the structural natural frequency (0.54 Hz), triggering efficient seismic energy transfer; the suspended slabs' weak vertical stiffness (connected only via hanger rods) further amplifies vibration amplitude. Second, the dynamic characteristics of the suspended substructure exacerbate the amplification effect. The suspended floor slabs, as independent mass units, exhibit obvious "mass-spring" system behavior in the vertical direction, with the hanger rods acting as elastic supports. The vertical seismic component directly excites this mass-spring system, and due to the low damping ratio of the system, energy dissipation is limited, causing continuous accumulation of vibration energy. Additionally, the suspended floor slabs are affected by higher-mode vibrations (as verified in the modal analysis in Section 2.4, where SSI prolongs higher-mode periods), and the vertical seismic component further amplifies these higher-mode responses, resulting in a superposition of fundamental mode and higher-mode accelerations that significantly increases the overall vertical acceleration.

First, resonance coupling between the NF-P ground motion and the suspended structure is the core driver. The dominant frequency of NF-P ground motions (0.61 Hz) is highly close to the structural natural frequency (0.54 Hz), triggering efficient seismic energy transfer; the suspended slabs' weak vertical stiffness (connected only via hanger rods) further amplifies vibration amplitude. Second, the dynamic characteristics of the suspended substructure exacerbate the amplification effect. The suspended floor slabs, as independent mass units, exhibit obvious "mass-spring" system behavior in the vertical direction, with the hanger rods acting as elastic supports. The vertical seismic component directly excites this mass-spring system, and due to the low damping ratio of the system, energy dissipation is limited, causing continuous accumulation of vibration energy. Additionally, the suspended floor slabs are affected by higher-mode vibrations (as verified in the modal analysis in Section 2.4, where SSI prolongs higher-mode periods), and the vertical seismic component further amplifies these higher-mode responses, resulting in a superposition of fundamental mode and higher-mode accelerations that significantly increases the overall vertical acceleration.

This phenomenon indicates that the amplification effect of the vertical seismic component on the vertical acceleration response exhibits pronounced nonlinear characteristics, with its amplification factor far exceeding that of the horizontal response. These findings reveal the directional sensitivity of the dynamic response of suspended substructures under multidimensional seismic coupling effects, suggesting that the control and optimization of vertical dynamic responses should be prioritized in the seismic design of suspended structures.

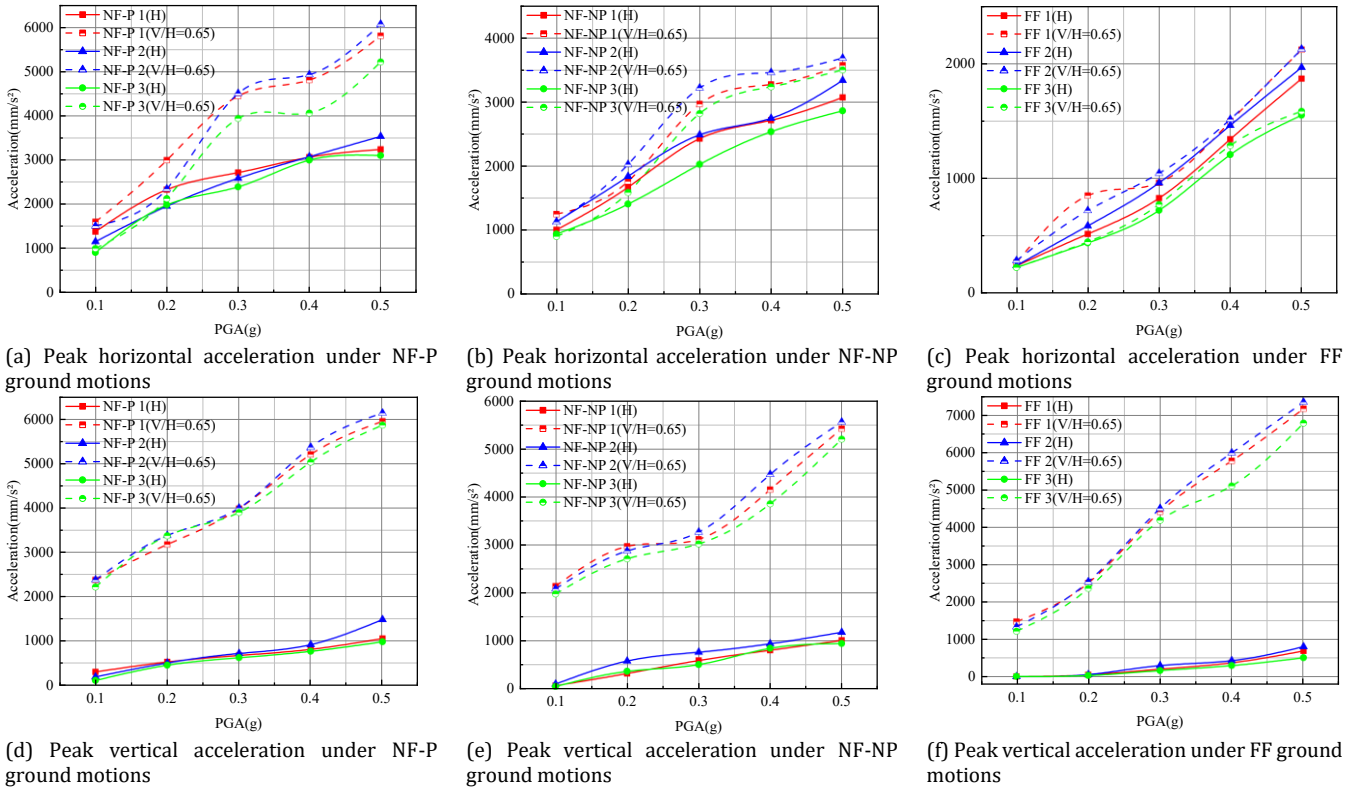

(a) Peak horizontal acceleration under NF-P ground motions

(b) Peak horizontal acceleration under NF-NP ground motions

(c) Peak horizontal acceleration under FF ground motions

(d) Peak vertical acceleration under NF-P ground motions

(e) Peak vertical acceleration under NF-NP ground motions

(f) Peak vertical acceleration under FF ground motions

Fig. 12 Effect of vertical earthquakes on the peak acceleration of the suspended floor slab

4.5 Hanger Rod Stress

The axial peak stress response characteristics of the top-floor hanger rods in the suspended structure under horizontal ground motions only and combined horizontal-vertical ground motions (with the vertical component scaled to 0.65 times the horizontal component) are illustrated in Fig. 13. The three ground motions considered have a uniform peak ground acceleration (PGA) of 0.1 g. The mean peak stress of the hanger rods increases when the vertical seismic component is considered. Under NF-P, NF-NP, and FF ground motions, the peak stress increases by 19%, 7.6%, and 8.2%, respectively. NF-P ground motion, containing long-period velocity pulses, transmits high-frequency vibration energy into the hanger rod-suspended mass system through their vertical component, resulting in significant stress amplification. This finding demonstrates that the vertical seismic component cannot be neglected in the seismic design of multi-story suspended floors system, particularly under NF-P ground motions, where its impact on structural stress responses is notably pronounced. Therefore, rational consideration of vertical seismic effects is critical for ensuring the safety of connection members in suspended structures.

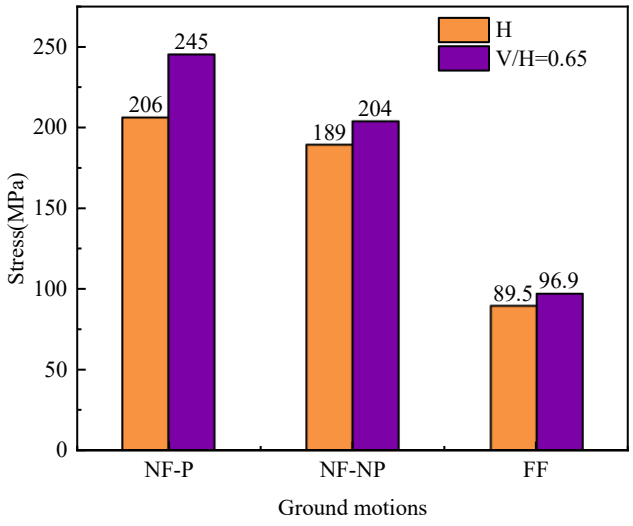

Fig. 13 Effect of vertical earthquakes on the axial peak stress of the top-level suspension hanger rod

5. Conclusions

An integrated model of a multi-story suspended floors system considering SSI was established, and its seismic responses under various types of multidimensional seismic excitations were investigated, with a focus on the pulse effects on the superstructure. The main conclusions are summarized as follows:

(1) SSI alters the dynamic characteristics of the suspended structure, leading to an extension of the natural vibration period, particularly in higher modes. Modal analysis reveals that the displacement pattern of suspended floor slabs in the proposed suspended structural system exhibits characteristics analogous to those of lumped masses in conventional shear-type structures, while the primary structural frame demonstrates minimal deformation.

(2) The vertical seismic component amplifies both the vertical displacement and the vertical acceleration responses of the suspended structure. At a PGA of 0.5 g, under NF-P ground motions, the mean vertical displacement and mean acceleration of the main structure increase by 2.64 times and 2.8 times, respectively, when the vertical seismic component is considered. The suspended floor slabs exhibit even greater sensitivity, with mean vertical acceleration amplification reaching 5.05 times, demonstrating pronounced direction-dependent response in the system's dynamic response. The growth rate of these responses far exceeds the simple linear superposition of seismic input intensities.

(3) Horizontal responses, including displacements and accelerations, are primarily governed by the horizontal seismic component inputs, with amplification factors ranging from 1.08 to 1.73 when including the vertical seismic component. Furthermore, under NF-P ground motions (0.61 Hz), which align closely with the structure's natural frequencies, the structural response is exacerbated, leading to higher risks of resonance.

(4) The axial stress in hanger rods increases notably due to vertical seismic coupling, with a 19% increase under NF-P ground motions at 0.1 g PGA, compared to horizontal-only cases. As hanger rods serve as the primary connection members, adequate safety margins should be reserved in their design to accommodate the effects of vertical seismic actions.

(5) Among the ground motion types, NF-P excitations produce the most severe responses due to their low-frequency content and velocity pulses, followed by NF-NP and FF ground motions. The emphasis on integrating SSI and vertical seismic effects into the seismic design of suspended structures, particularly in near-fault regions, is supported by the following key rationales: First, near-fault regions are dominated by NF-P ground motions, which are characterized by strong velocity pulses and low-frequency components (mean dominant frequency of 0.61 Hz in this study). These characteristics are highly compatible with the natural vibration frequency of suspended structures (0.54 Hz), easily triggering resonance effects and significantly amplifying vertical displacements, accelerations, and hanger rod stresses. Second, the flexible connection form of suspended structures makes them more sensitive to vertical seismic inputs, leading to nonlinear amplification of vertical responses. Third, SSI has a more significant impact on structural dynamic characteristics in near-fault regions: the low-frequency components of NF-P ground motions interact with the soil's flexible constraints, further prolonging the structural natural period and increasing the resonance risk. In contrast, far-field ground motions are dominated by high-frequency components (mean dominant frequency of 9.06 Hz) that are less compatible with the structural natural frequency, and their vertical seismic intensities are relatively weak, resulting in less severe structural responses. Therefore, integrating SSI and vertical seismic effects into design codes for suspended structures in near-fault regions is critical to ensuring structural robustness and seismic safety.

Acknowledgements

We would like to acknowledge the Suqian Sci & Tech Program (Grant No. H202412) for the support and help provided in this paper.

Conflict of Interest

The authors declare that there is no conflict of interest regarding the publication of this paper.

References

Abdelhalim, A., El Naggar, M.H., Kim, K., Hussein, A.F., & Elgamal, A. (2025). Seismic performance and soil-structure interaction of shallow reinforced concrete tunnels. Soil Dynamics and Earthquake Engineering, 194, 109372. https://doi.org/10.1016/j.soildyn.2025.109372 https://doi.org/10.1016/j.soildyn.2025.109372

Applied Technology Council. (2009). Quantification of Building Seismic Performance Factors: FEMA P695. Federal Emergency Management Agency.

Cao, W., Lu, Z., Zhang, J., Chang, W., & Zhang, C. (2007). Shaking table test and analysis of core-tube partial suspension structures. China Civil Engineering Journal, 40(03), 40-44 and 82. https://doi.org/10.15951/j.tmgcxb.2007.03.007

Chen, M., Liang, X., Yang, Z., Ge, X., & Xu, C. (2023). Analytical study on the random seismic responses of an asymmetrical suspension structure. Buildings, 13(6), 1435. https://doi.org/10.3390/buildings13061435

Chopra, A.K. (2017). Dynamics of Structures: Theory and Applications to Earthquake Engineering. Pearson Education, Inc, Hoboken, New Jersey.

Chulahwat, A., & Mahmoud, H. (2017). A combinatorial optimization approach for multi-hazard design of building systems with suspended floor slabs under wind and seismic hazards. Engineering Structures, 137, 268-284. https://doi.org/10.1016/j.engstruct.2017.01.074

Du, L., Zhang, W., Tu, Y., Song, S., Sas, G., & Elfgren, L. (2022). Shaking table test on a novel mega-frame suspended structural system. Journal of Building Engineering, 52, 104440. https://doi.org/10.1016/j.jobe.2022.104440

Guo, Y., Pei, Y., & Li, Z. (2003). Seismic response analysis of high-rise building with suspended structure system. Journal of Chongqing Jianzhu University, 25(05), 42-46 and 74.

He, Q., Yin, A., Fan, Z., & He, L. (2020). Seismic responses analysis of multi-story suspended floors system. Journal of Vibroengineering, 23(1), 167-182. https://doi.org/10.21595/jve.2020.21478

Islam, M.R., Turja, S.D., Nguyen, D.V., Kim, D., & Choo, Y.W. (2024). Seismic behavior of soil-tunnel-building system considering earthquake frequency contents. Journal of Building Engineering, 97, 110892. https://doi.org/10.1016/j.jobe.2024.110892

Liang, S., Sun, X., Zhong, X., Hu, R., Zhu, X., & Xu, J. (2025). Suspension structure design and intelligent construction of a civic center project. Building Science, 41(01), 136-144. https://doi.org/10.13614/j.cnki.11-1962/tu.2025.01.015

Liu, X., Wang, W., & Fang C. (2022). Seismic vibration control of novel prefabricated industrial equipment suspension structures with tuned mass damper. Journal of Constructional Steel Research, 191, 107163. https://doi.org/10.1016/j.jcsr.2022.107163

Lu, H., Liang, P., & Shang, S. (2007). Computational analysis of dynamic layered soil-pile-structure interaction. Chinese Journal of Geotechnical Engineering, 29(05), 705-711.

Mahmoud, H., & Chulahwat, A. (2015). Response of building systems with suspended floor slabs under dynamic excitations. Engineering Structures, 104, 155-173. https://doi.org/10.1016/j.engstruct.2015.09.027

Ministry of Housing and Urban-Rural Development & General Administration of Quality Supervision, Inspection and Quarantine. (2010). Code for Seismic Design of Buildings GB 50011-2010 [S]. Beijing: China Architecture & Building Press.

Naderpour, H., SoltaniMatin, A., Kheyroddin, A., Fakharian, P., & Ezami, N. (2024). Optimizing Seismic Performance of Tuned Mass Dampers at Various Levels in Reinforced Concrete Buildings. Buildings, 14(8), 2443. https://doi.org/10.3390/buildings14082443

Ozturk, B., Cetin, H., & Aydin, E. (2022). Optimum vertical location and design of multiple tuned mass dampers under seismic excitations. Structures, 41, 1141-1163. https://doi.org/10.1016/j.istruc.2022.05.014

Pasand, A.A., & Zahrai, S.M. (2024). Seismic control of tall buildings using vertically distributed multiple tuned mass dampers. The Structural Design of Tall and Special Buildings, 33(14), e2123-e2123. https://doi.org/10.1002/tal.2123

Wang, C., Lyu, Z., & Wu, J. (2008a). Analysis of the mechanism and efficiency of vibration-absorption for semi-flexible suspension systems. China Civil Engineering Journal, 41(01): 48-54. https://doi.org/10.15951/j.tmgcxb.2008.01.010

Wang, C., Lyu, Z., & Wu, J. (2008b). Seismic response of semi-flexible suspension vibration-absorption structures. Journal of Building Structures, 29(06), 107-112. https://doi.org/10.14006/j.jzjgxb.2008.06.007

Wei, X., Liu, S., Ma, F., & Zhang J. (2013). The impact analysis of vibration-suppressed effectiveness of core-wall suspension isolation structure caused by dynamic parameter. Industrial Construction, 43(02), 34-38 and 58.

Wolf, J.P. (1985). Dynamic Soil-Structure Interaction. Prentice-Hall, Inc, Englewood Cliffs, New Jersey.

Xiao, K., Jia, S., Jia, J., & Gu, X. (2022). Design and research on suspended structure scheme of Shanghai East Library. Building Structure, 52(1), 1-6. https://doi.org/10.19701/j.jzjg.20200521

Yang, F., Zhao, H., Ma, T., Bao, Y., Cao, K., & Li X. (2024). Three-Dimensional numerical analysis of seismic response of steel frame-core

wall structure with basement considering soil-structure interaction effects. Buildings, 14(11), 3522. https://doi.org/10.3390/buildings14113522

Yang, K., Cai, P., Zhang, Z., Hou, Q., Zheng, R., Hao, B., & Wang, B. (2024). Effects of soil-structure interaction on the seismic response of RC frame-shear wall building structures under far-field long-period ground motions. Buildings, 14(12), 3796. https://doi.org/10.3390/buildings14123796

Ye, Z., Feng, D., & Wu, G. (2019). Seismic control of modularized suspended structures with optimal vertical distributions of the secondary structure parameters. Engineering Structures, 183, 160-179. https://doi.org/10.1016/j.engstruct.2018.12.099

Ye, Z., Wu, G., Feng D., & Shafieezadeh, A. (2020). Shake table testing and computational investigation of the seismic performance of modularized suspended building systems. Bulletin of Earthquake Engineering, 18(11), 5247-5279. https://doi.org/10.1007/s10518-020-00902-3

Yin, A. (2020). Seismic performance analysis of multi-story suspended floors system based on Matlab numerical model. Lanzhou University of Technology.

Zhou, J., & Wu, X. (2005b). Study on core-wall suspension structure Ⅱ: theoretical analysis. Journal of Beijing Institute of Civil Engineering and Architecture, 21(04), 1-8 and 23.

Zhou, J., Wu, X., & Liu, N. (2005a). Study on core-wall suspension structure Ⅰ: shaking table test. Journal of Beijing Institute of Civil Engineering and Architecture, 21(03), 4-9 and 25.

Disclaimer